

Train Once for All: A Transitional Approach for Efficient Aspect Sentiment Triplet Extraction

Xinmeng Hou¹ Lingyue Fu² Chenhao Meng² Hai Hu^{2*}

¹Columbia University, New York, NY, USA

²Shanghai Jiao Tong University, Shanghai, China
fh2450@tc.columbia.edu

fulingyue@sjtu.edu.cn, chenhaomeng@sjtu.edu.cn, hu.hai@sjtu.edu.cn

Abstract

Aspect-Opinion Pair Extraction (AOPE) and Aspect Sentiment Triplet Extraction (ASTE) have gained significant attention in natural language processing. However, most existing methods are a pipelined framework, which extracts aspects/opinions and identifies their relations separately, leading to a drawback of error propagation and high time complexity. Towards this problem, we propose a transition-based pipeline to mitigate token-level bias and capture position-aware aspect-opinion relations. With the use of a fused dataset and contrastive learning optimization, our model learns robust action patterns and can optimize separate subtasks jointly, often with linear-time complexity. The results show that our model achieves the best performance on both the ASTE and AOPE tasks, outperforming the state-of-the-art methods by at least 6.98% in the F1 measure. The code is available at https://github.com/Paparare/trans_aste.

1 Introduction

Aspect-Based Sentiment Analysis (ABSA) is a fine-grained sentiment analysis task that identifies specific aspects in text and analyzes the sentiments linked to them. It involves subtasks such as: **Aspect Extraction (AE)**: Identifying mentioned aspects. **Opinion Extraction (OE)**: Extracting opinion terms related to aspects. **Aspect-Opinion Pair Extraction (AOPE)**: Extracting aspect-opinion pairs. **Aspect-Sentiment Triplet Extraction (ASTE)**: Identifying aspect, opinion, and sentiment polarity triplets.

Classic ABSA approaches often use a pipeline architecture, performing subtasks like aspect extraction (AE) and opinion extraction (OE) separately. For instance, in the sentence: “*Gourmet food is delicious. Good service, but not so welcoming.*” AE identifies **gourmet food** and **service** as aspects, while OE extracts **delicious**, **good**,

*Corresponding author

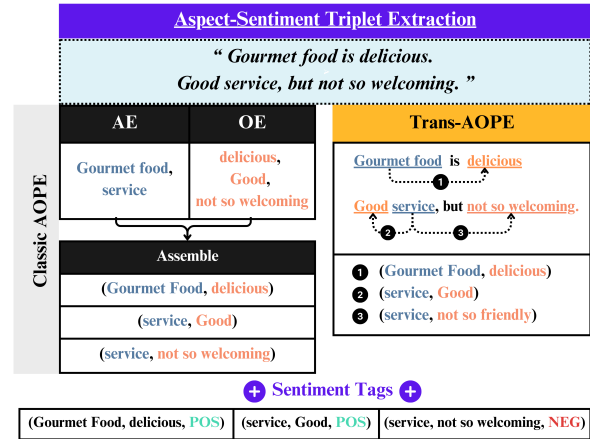


Figure 1: For the sentence 'Gourmet food is delicious. Good service, but not so welcoming,' this example demonstrates the processing steps in both classic and transitional methods for extracting aspect-opinion pairs and tagging sentiment polarity. AE stands for Aspect Extraction, OE for Opinion Extraction, POS represents positive sentiment, and NEG represents negative sentiment.

and **not so welcoming** as opinions. These outputs are combined to form aspect-opinion pairs, with sentiment tagging assigning polarities to create triplets. Past studies have generally achieved satisfactory performance on aspect and opinion extraction (Jiang et al., 2023; Wang et al., 2023; Chakraborty, 2024). Adding the according sentiment tags with pair, ASTE is the most integrated task for aspect-based sentiment analysis that has seen the development of diverse models leveraging various methodologies. Pipeline-based approaches, such as Peng-Two-stage (Peng et al., 2020), decompose the task into multiple stages for modular refinement. Sequence-to-sequence frameworks like BARTABSAs (Yan et al., 2021) employ pre-trained transformers to generate triplets flexibly. Sequence-tagging methods, including GTS (Wu et al., 2020) and JET-BERT (Xu et al., 2020), annotate tokens for precise identification of relation-

ships. Machine Reading Comprehension (MRC)-based models, such as COM-MRC (Zhai et al., 2022) and Triple-MRC (Zou et al., 2024), reframe the task as query answering for efficient extraction. Graph-based approaches such as EMC-GCN (Chen et al., 2022), BDTF (Chen et al., 2022), and DGC-NAP (Li et al., 2023) use graph structures to capture semantic and syntactic interactions. Tagging schema-based models, exemplified by STAGE-3D (Liang et al., 2023), use hierarchical schemas for multi-level extraction, while lightweight models like MiniConGTS (Sun et al., 2024) focus on efficiency with reduced computational costs.

Although previous studies have shown satisfactory results for individual entity extraction, performance on pair and triplet extraction remains suboptimal, with state-of-the-art (SOTA) scores in the 60s and 70s (Sun et al., 2024). Two key challenges contribute to this gap: (1) *Disconnected Aspect-Opinion Extraction*: Opinions are often extracted independently from their corresponding aspects in previous studies (Liang et al., 2023; Sun et al., 2024). While relationships can be added as an auxiliary factor to assist pair extraction (Liu et al., 2022; Wang et al., 2023), this approach loses critical contextual information by treating aspects and opinions as separate entities. This limits the effectiveness of many token-based extraction methods. (2) *Time Complexity with Longer Sequences*: Methods using 2D matrix tagging (Liang et al., 2023; Sun et al., 2024) to capture relationships between tokens face significant increases in time complexity as the length of the token sequence increases. This computational burden restricts their scalability, especially for longer texts in practical applications.

As an overview, the critical contributions of our study are as follows:

Efficient Transition Pipeline for AOPE: We propose a transition pipeline for simultaneous aspect-opinion pair extraction, achieving linear time complexity $O(n)$.

Augmented Learning for Model Optimization: Building on this transitional backbone, we introduce a contrastive-augmented optimization method to enhance model efficiency.

New SOTA Performance on AOPE and ASTE: Our model achieves new state-of-the-art (SOTA) performance on both AOPE and ASTE tasks.

2 Related Work

2.1 Transition-based Methods

Transition-based approaches are widely used in dependency parsing, leveraging shift-reduce and bidirectional arc actions (left-arc, right-arc) for efficient $O(n)$ parsing (Aho and Ullman, 1973; Nivre, 2003; Cer et al., 2010). These parsers maintain stack, buffer, and arc relations to track transitions and have been extended to tasks like token segmentation (Zhang et al., 2016) and argument mining (Bao et al., 2021). Beyond parsing, transition-based methods have been applied to structured sentiment analysis, generating graph structures for opinion extraction (Fernández-González, 2023) and incremental constituency parsing using graph neural networks (Yang and Deng, 2020). A unifying theory bridges transition-based parsing and sequence labeling for simplified learning (Gómez-Rodríguez et al., 2020), while in AMR parsing, structure-aware fine-tuning achieves state-of-the-art results (Zhou et al., 2021). Their flexibility and efficiency make them effective across diverse NLP tasks.

2.2 Contrastive-based Optimization

Contrastive learning has demonstrated its effectiveness in various domains, achieving state-of-the-art results in token-independent extraction tasks with models such as MINIconGTS (Sun et al., 2024). Recent works have further explored its potential: contrastive learning for prompt-based few-shot language learners enhances generalization through augmented "views" (Jian et al., 2022); contrastive learning as goal-conditioned reinforcement learning provides a novel loss function with theoretical guarantees for improved success in goal-directed tasks (Eysenbach et al., 2023), and studies analyzing the role of margins reveal critical factors like positive sample emphasis for better generalization (Rho et al., 2023). These advances showcase contrastive learning's flexibility and robustness, which inspired us to integrate it into our transition-based AOPE and ASTE to refine representation learning and improve model performance.

3 Methodology

In this section, we introduce a novel paradigm that integrates the extraction of aspect-opinion pairs into a process reminiscent of constructing a parsing-directed graph. This model progressively constructs and annotates aspect-oriented relations us-

Action	Symbolic Expression
Shift (SF)	$(\sigma_0, \beta_0 \mid \beta_1, E, C, R) \xrightarrow{SF} (\sigma_0 \mid \sigma_1, \beta_1, E, C, R)$
Stop (ST)	$(\sigma_0, A, O, R) \xrightarrow{ST} (\sigma_0, A, O, R)$
Merge (M)	$(\sigma_0 \mid \sigma_1, \beta_1 \mid \beta_2, A, O, R) \xrightarrow{M} (\sigma_{0\&1}, \beta_1 \mid \beta_2, A, O, R)$
Left Constituent Removal (L_n)	$(\sigma_0 \mid \sigma_1, \beta_0, A, O, R) \xrightarrow{L_n} (\sigma_1, \beta_0, A, O, R)$
Right Constituent Removal (R_n)	$(\sigma_0 \mid \sigma_1, \beta_0, A, O, R) \xrightarrow{R_n} (\sigma_1, \beta_0, A, O, R)$
Left-Relation Formation (LR)	$(\sigma_0 \mid \sigma_1, \beta_0, A, O, R) \xrightarrow{LR} (\sigma_0 \mid \sigma_1, \beta_0, A \cup \sigma_1, O \cup \sigma_0, R \cup \sigma_0 \leftarrow \sigma_1)$
Right-Relation Formation (RR)	$(\sigma_0 \mid \sigma_1, \beta_0, E, C, R) \xrightarrow{RR} (\sigma_0 \mid \sigma_1, \beta_0, A \cup \sigma_0, O \cup \sigma_0, R \cup \sigma_0 \rightarrow \sigma_1)$

Table 1: Symbolic Expressions for the Proposed Actions.

ing input sequences enriched with contextual features. Unlike the classic approach, which employs three sets to record action histories, we utilize five sets, including stack, buffer, aspect, and pair, to show how aspect and opinion are extracted simultaneously.

3.1 Transitional Operations and State Change

The construction of relationships between phrases is achieved through systematic transition actions, conceptualized as directed edges linking two nodes (tokens), N_1 and N_2 . A relationship transitioning N_1 to N_2 under relation l_1 is denoted as $RR = N_1 \xrightarrow{l_1} N_2$ or $LR = N_1 \xleftarrow{l_1} N_2$, representing aspect-oriented direction. To interpret causal links, l_1 is defined as l_L or l_R for bidirectional relations. Opinion constituents (E_1) may precede or follow aspect constituents, which can span multiple tokens (e.g., “gourmet food,” “not bad”). This requires additional steps to consolidate multi-token constituents. For the ASTE task, we define seven distinct transition actions that combine token retrieval, termination, and token merging.

The action framework aims to prevent information leakage and ensure flexibility in relation arching. Actions are recorded as tuples $T = (\sigma, \beta, A, O, R)$, representing the stack, buffer, aspect, opinion, and relation. The ASTE task includes default actions, which are universal and required for all data, primary actions that handle merging or removal, and secondary actions for relation arching, which depend on the outcomes of the primary actions. Verbal and symbolic representations of state transitions for each action are provided below.

Default Actions:

1. **Shift** (SF) moves a token from the tokenized stack into the buffer for further processing.
2. **Stop** (ST) halts the process when only one

token remains in the buffer, and the stack is empty.

Primary Actions:

1. **Merge** (M) combines multiple tokens in the buffer into a single compound target.
2. **Left Constituent Removal** (L_n) removes the left constituent from the buffer.
3. **Right Constituent Removal** (R_n) removes the right constituent from the buffer.

Secondary Actions:

1. **Left-Relation Formation** (LR) creates a relation from the right aspect constituent to the left opinion constituent.
2. **Right-Relation Formation** (RR) creates a relation from the left aspect constituent to the right opinion constituent.

Table 1 provides a symbolic illustration of how the symbolic state is constructed and utilized. Take the sentence "Gourmet food is delicious" as an example. Table 2 demonstrates the process of moving tokens from the buffer to the stack, deciding whether they should be merged into a single entity or removed, and finally evaluating them for relation formation. It is important to note that the set of actions shown in the figure is not the only way to extract the "Gourmet food" and "delicious" aspect-opinion pair. The alternative solution for parsing the sentence is shown in Appendix 5.

3.2 Trans-AOPE State Representation

The model we propose consists of two core stages: pair extraction with a designed transitional action slot (in purple) and pair-based sentiment tagging (in orange), as illustrated in Figure 2.

In the first stage, the input, denoted as $I_1^n = (t_1, t_2, \dots, t_n)$, is a sequence of tokens. The output is a sequence of actions, represented as $A_1^m =$

Phrase	Action	Stack (σ)	Buffer (β)	Aspect	Opinion	Pair
–	–	$[\]$	$[\beta_1, \beta_2, \beta_3, \beta_4]$	–	–	–
1	SF	$[\sigma_1]$	$[\beta_2, \beta_3, \beta_4]$	–	–	–
2	SF	$[\sigma_1, \sigma_2]$	$[\beta_3, \beta_4]$	–	–	–
3	M	$[\sigma_{1\&2}]$	$[\beta_3, \beta_4]$	–	–	–
4	SF	$[\sigma_{1\&2}, \sigma_3]$	$[\beta_4]$	–	–	–
5	R_n	$[\sigma_{1\&2}]$	$[\beta_4]$	–	–	–
6	SF	$[\sigma_{1\&2}, \sigma_4]$	$[\]$	–	–	–
7	RR	$[\sigma_{1\&2}, \sigma_4]$	$[\]$	$[\sigma_{1\&2}]$	$[\sigma_4]$	$(\sigma_{1\&2} \rightarrow \sigma_4)$
9	ST	$[\]$	$[\]$	$[\sigma_{1\&2}]$	$[\sigma_4]$	$(\sigma_{1\&2} \rightarrow \sigma_4)$

Table 2: State changes for "Gourmet food is delicious" using symbolic representation. Here, σ_1 corresponds to "Gourmet", σ_2 to "food", σ_3 to "is", and σ_4 to "delicious". Similarly, $\beta_1, \beta_2, \beta_3,$ and β_4 correspond to tokens in the buffer in sequence.

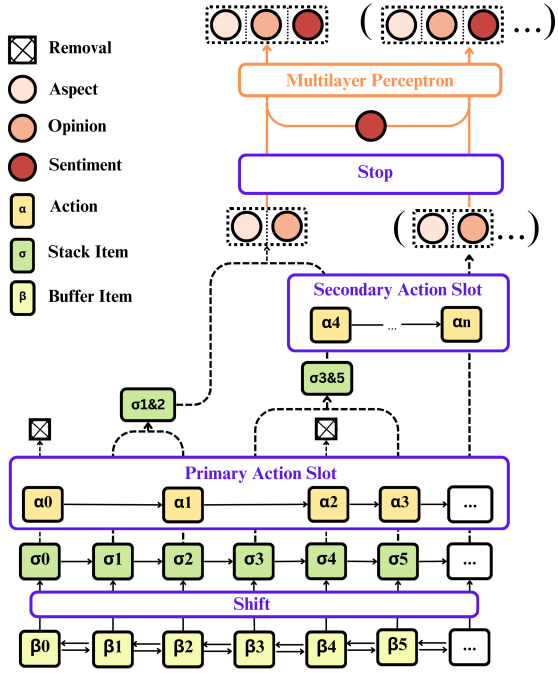


Figure 2: The complete process of the transition-based model is illustrated. Purple highlights represent the transition-based pair extraction, while orange indicates the final step of sentiment tagging.

(a_1, a_2, \dots, a_m) . This process can be conceptualized as a search for the optimal action sequence, A^* , given the input sequence I_1^n . At each step n , the model predicts the next action based on the current system state, S , and the sequence of prior actions, A_1^{n-1} . The updated system state, S_{n+1} , is determined by the specific action a_t . We define r_n as a symbolic representation for calculating the probability of the action a_n at step n . This probability is computed as follows:

$$p(a_n|r_n) = \frac{\exp(w_{a_n}^\top r_n + b_{a_n})}{\sum_{a' \in \mathcal{A}(S)} \exp(w_{a'}^\top r_n + b_{a'})} \quad (1)$$

Here, w_a is a learnable parameter vector, and b_a is a

bias term. The set $\mathcal{A}(S)$ represents the legal actions available given the current parser state. The overall optimization objective for the model is defined as:

$$\begin{aligned} (A^*, S^*) &= \operatorname{argmax}_{A, S} \prod_n p(a_n, S_{n+1} | A_1^{n-1}, S_n) \\ &= \operatorname{argmax}_{A, S} \prod_n p(a_n | r_n) \end{aligned} \quad (2)$$

In this stage, the ASTE task is incorporated into a transition-based action prediction task. In order to decode efficiently, the action boasting the maximum probability is chosen through a greedy approach until the parsing procedure reaches a point of termination. This model thus forms the basis of an efficient transition-based prediction system that utilizes a representation of the current system state and action history to generate the most likely subsequent action at each step in a sequence. By integrating these concepts, the model successfully carries out parsing tasks while avoiding information leakage and ensuring flexibility in the relation arching process.

3.3 Transition Implementation with Neural Model

This section outlines the transition-based parsing process using neural models. RoBERTa (Liu et al., 2019) encodes textual phrases, while UniLSTM (Hochreiter and Schmidhuber, 1997) and BiLSTM (Graves and Schmidhuber, 2005) model dynamic transitions. The parser state is initialized and evolves through a sequence of actions with distributed embeddings and LSTMs representing the state at each step. At the end stage, a Multi-Layer Perceptron (MLP) is employed to classify the sentiment associated with each pair or triplet based on the evolved parser state.

Token representations Consider the process of parsing a text $d_1^n = (p_1, p_2, \dots, p_n)$, consisting of n phrases. Each phrase $p_i = (w_{i1}, w_{i2}, \dots, w_{il})$ contains l tokens. A phrase can be represented as a sequence $x_i = ([CLS], t_{i1}, \dots, t_{il}, [SEP])$, where [CLS] is a special classification token whose final hidden state serves as the aggregate sequence feature, and [SEP] is a separator token. The hidden representation of each phrase is computed as $h_{p_i} = \text{RoBERTa}(x_i) \in \mathbb{R}^{d_b \times |l_i|}$, where d_b is the hidden dimension size, and $|l_i|$ is the length of the sequence x_i . Finally, the entire text d_1^n is represented as a list of tokens: $h_d = [h_{p_1}, h_{p_2}, \dots, h_{p_n}]$.

State Initialization At the start of the parsing process, the parser’s state is initialized as ($\beta = \emptyset, \sigma = [1, 2, \dots, n], E = \emptyset, C = \emptyset, R = \emptyset$), where σ is the stack, β is the buffer, and E, C , and R are empty sets representing different outputs. The state evolves through a sequence of actions, progressively consuming elements from the buffer β and constructing the output. This process continues until the parser reaches its terminal state when there is only one token left in buffer, represented as ($\beta = [SEP], \sigma = \emptyset, E, C, R$).

Step-by-Step Parser State Representation. For the action sequence, each action a is mapped to a distributed representation e_a through a lookup table E_a . A unidirectional LSTM is then utilized to capture the complete history of actions in a left-to-right manner at each step t :

$$\alpha_t = \text{LSTM}_a(a_0, a_1, \dots, a_{t-1}, a_t) \quad (3)$$

Upon generation of a new action a_t , its corresponding embedding e_{a_t} is integrated into the rightmost position of LSTM_a . To further refine the representation of the pair (σ_1, σ_0) , their relative positional distance d is also encoded as an embedding e_d from a lookup table E_d . The composite representation of the parser state at step t encompasses these varied features.

The parser state is represented as a triple (β_s, σ_s, A_t) , where σ_s denotes the stack sequence $(\sigma_0, \sigma_1, \dots, \sigma_n)$, β_s represents the buffer sequence $(\beta_0, \beta_1, \dots, \beta_n)$, and A_t encapsulates the action history $(a_0, a_1, \dots, a_{t-1}, a_t)$. The stack (σ_n) and buffer (β_n) are encoded using bidirectional LSTMs as follows:

$$[s_t, b_t] = \text{BiLSTM}((\sigma_n, \beta_0), (\sigma_{n-1}, \beta_1), \dots, (\sigma_0, \beta_n)) \quad (4)$$

Here, s_t and b_t are the output feature representations of the stack and buffer, respectively. Each of these representations consists of forward and backward components: $\sigma_t = (\overrightarrow{\sigma}_t, \overleftarrow{\sigma}_t)$ and $\beta_t = (\overrightarrow{\beta}_t, \overleftarrow{\beta}_t)$. The forward and backward components are matrices in $\mathbb{R}^{d_l \times |\sigma_t|}$ and $\mathbb{R}^{d_l \times |\beta_t|}$, respectively, where d_l is the hidden dimension size of the LSTM, and $|\sigma_t|, |\beta_t|$ are the lengths of the sequences σ_t and β_t .

3.4 Optimization Implementation

We compare two optimization strategies: regular optimization using Cross-Entropy Loss and contrastive-based optimization, which aligns predicted and true action embeddings. A weight study will evaluate the impact of the positioning of two components in augmented optimization on model performance.

3.4.1 Base Optimization

Both action and sentiment classification tasks are optimized using the Cross-Entropy Loss as base optimization, defined as follows:

$$\mathcal{L} = -\frac{1}{N} \sum_{i=1}^N \sum_{j=1}^M y_i^j \log(p_i^j), \quad (5)$$

where N is the number of samples, M is the number of classes (either action or sentiment classes), y_i^j is a binary indicator (0 or 1) indicating whether class j is the correct class for sample i , and p_i^j is the predicted probability for class j for sample i . The total loss is the sum of the losses for both tasks:

$$\mathcal{L}_{\text{base}} = \mathcal{L}_{\text{action}} + \mathcal{L}_{\text{sentiment}}. \quad (6)$$

3.4.2 Contrastive-based Optimization

Given the predicted action logits $\mathbf{A}_{\text{logits}}$ and the true action labels \mathbf{A}_{true} , the predicted actions are obtained by applying a softmax function followed by an argmax:

$$\mathbf{A}_{\text{pred}} = \text{argmax}(\text{softmax}(\mathbf{A}_{\text{logits}}))$$

The predicted and true actions are then embedded as follows:

$$\mathbf{E}_{\text{pred}} = \text{Embed}(\mathbf{A}_{\text{pred}}), \quad \mathbf{E}_{\text{true}} = \text{Embed}(\mathbf{A}_{\text{true}})$$

For each sample i , compute the cosine similarity between $\mathbf{E}_{\text{pred}}^{(i)}$ and all $\mathbf{E}_{\text{true}}^{(j)}$ to form a similarity matrix. Using this matrix, the diagonal elements

represent positive pairs, while the non-diagonal elements represent negative pairs.

Next, calculate the positive and negative cosine similarities, and apply the exponential function:

$$e_{\text{pos}} = \exp(\text{cos_sim}(\mathbf{E}_{\text{pred}}, \mathbf{E}_{\text{true}}) \cdot \mathbf{M}_{\text{pos}}) \quad (7)$$

$$e_{\text{all}} = \exp(\text{cos_sim}(\mathbf{E}_{\text{pred}}, \mathbf{E}_{\text{true}})) \quad (8)$$

where, cos_sim denote cosine similarity function \mathbf{M}_{pos} is a mask that selects only positive pairs (diagonal entries).

Now compute the contrastive loss as:

$$\mathcal{L}_{\text{con}} = -\frac{1}{N} \sum_{j=1}^N \log \left(\frac{\exp_{\text{pos}}^{(j)}}{\exp_{\text{all}}^{(j)}} \right) \quad (9)$$

Finally, the total loss is computed as:

$$\mathcal{L}_{\text{total}} = \omega_1 \cdot \mathcal{L}_{\text{base}} + \omega_2 \cdot \mathcal{L}_{\text{con}} \quad (10)$$

where ω are weighting factors, and $\mathcal{L}_{\text{base}}$ represents any regularization loss added to improve model generalization.

4 Experiments

4.1 Dataset

We used well-established benchmarks in Sentiment Analysis: SemEval 2014 (**14lap**, **14res**) (Pontiki et al., 2014), SemEval 2015 (**15res**) (Pontiki et al., 2015), and SemEval 2016 (**16res**) (Pontiki et al., 2016). These datasets, originally curated for the Semantic Evaluation (SemEval) competitions, are widely used for aspect-based sentiment analysis and extraction tasks (Xu et al., 2021).

We employed a data processing framework to construct sentiment-enhanced dependency graphs for ASTE datasets. This framework utilizes SpaCy (Honnibal et al., 2020) to extract syntactic dependencies and integrates sentiment scores from SenticNet (Cambria et al., 2017) to generate weighted adjacency matrices. These enriched graph representations aim to expand the feature space and reduce biased learning. Along with tokenized sentences and their corresponding aspect-opinion-sentiment triplets, the processed data supports downstream tasks, including model training and evaluation.

We evaluated the conformity of our transition operations in extracting aspects and opinions, with action evaluation results listed in Appendix A.3. Since our approach predicts actions rather than tokens, we assessed how well the model learns action patterns across individual datasets. For instance,

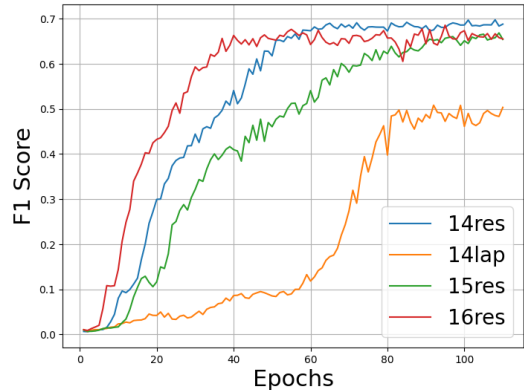


Figure 3: F1 Score over epochs for the model trained on 14res, 14lap, 15res, and 16res datasets and tested on the 15res dataset. The results indicate that training on datasets other than 15res, such as 14res can yield an even better performance, which suggests the presence of richer action patterns in other datasets for the model to learn.

as shown in Figure 3, the model did not perform best on the 15res test set when trained on the 15res training set. This suggests that other datasets, such as 14res, may contain richer action patterns for the model to learn. Consequently, we believe that training on a fused dataset provides a more diverse context, enhancing the model’s ability to learn these actions, which we then evaluated on separate test sets.

4.2 Baselines

We use two baselines: published scores from prior studies and previous SOTA models run on the fused dataset. Regular baselines include classic attention-based methods (e.g., *CMLA* (Wang et al., 2017)), pipeline approaches (*Peng-Two-stage* (Peng et al., 2020)), sequence-to-sequence frameworks (*BARTABSA* (Yan et al., 2021)), sequence-tagging methods (*GTS* (Wu et al., 2020), *JET-BERT* (Xu et al., 2020)), MRC-based models (*COM-MRC* (Zhai et al., 2022), *Triple-MRC* (Zou et al., 2024)), graph-based approaches (*EMC-GCN* (Chen et al., 2022), *DGCNAP* (Li et al., 2023)), and the SOTA *MiniConGTS* (Sun et al., 2024).

In addition to baselines on separate datasets, we selected two state-of-the-art models with publicly available and runnable code: the most recent model, *MiniConGTS* (Sun et al., 2024), and the earlier state-of-the-art for pair extraction, *BARTABSA* (Yan et al., 2021). We used their original configurations and data processing pipelines, modifying only the training data to include all four training sets

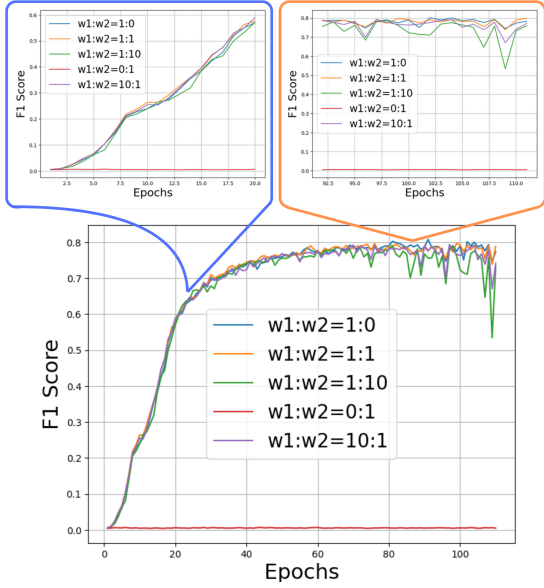


Figure 4: Growth on different weights for AOPE task on 14lap testing set.

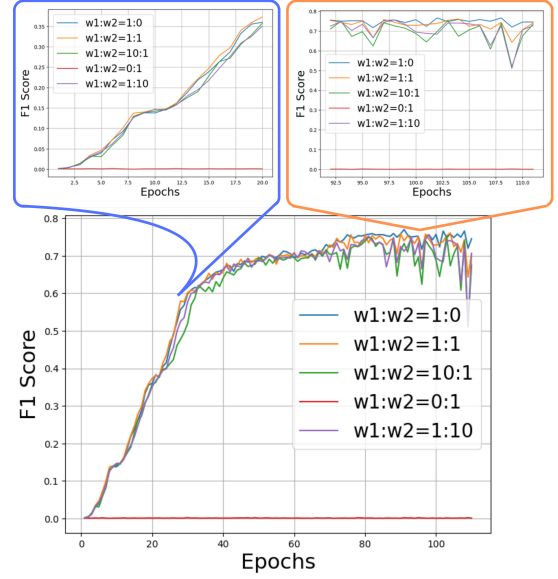


Figure 5: Growth on different weights for ASTE task on 14lap testing set.

from 14lap, 14res, 15res, and 16res. The models were then separately evaluated on the four corresponding test sets.

4.3 Results and Analysis

4.3.1 Study on Augmented Optimization

To assess the impact of weight compositions in Equation 10, we tested $(w_1, w_2) \in \{(1 : 0), (1 : 1), (1 : 10), (0 : 1), (10 : 1)\}$, where w_1 and w_2 are the weights for base and contrastive-based optimization, respectively, using a batch size of 4. Results for AOPE and ASTE are presented in Figures 4 and 5. For AOPE, contrastive-heavy weights ($w_1 : w_2 = 1 : 1$ and $w_1 : w_2 = 1 : 10$) performed well during early epochs (1–50), demonstrating the early advantages of contrastive optimization. After epoch 50, base ($w_1 : w_2 = 1 : 0$) and balanced ($w_1 : w_2 = 1 : 1$) optimizations provided greater stability and better final performance. In ASTE, base and balanced optimizations consistently outperformed others, indicating that ASTE primarily benefits from foundational learning, with limited advantages from contrastive optimization.

Similar trends were observed across other datasets, as shown in Appendix A.4, highlighting the broader applicability of these findings. Although contrastive-enhanced optimization does not deliver the best overall performance, it effectively improves efficiency in pair extraction tasks.

4.3.2 Comparison with Baselines

On AOPE As listed in Table 3, the F1 performance of Trans-AOPE demonstrates significant improvements over the baselines, particularly on the 14Res and 14Lap datasets. For 14Res, it achieves an absolute performance gain (APG)¹ of 10.51% compared to BARTABSA-fused and 6.66% over MiniConGTS-fused, highlighting its superior ability to balance precision and recall. Similarly, for 14Lap, the APG is 13.21% and 7.24%, respectively. In the 15Res dataset, the model achieves a marginal APG of 1.14% over BARTABSA-fused but falls slightly short of MiniConGTS-fused by -1.26%, reflecting potential limitations in handling highly specific cases. For 16Res, the model outperforms both baselines with an APG of 3.82% over BARTABSA-fused and 10.73% over MiniConGTS-fused.

On ASTE Results for ASTE are listed in Table 4. For the 14Res dataset, *Trans-ASTE* achieves the highest F1 score (84.44%), representing an APG of 12.76% over *BARTABSA-fused*. Similarly, it outperforms *MiniConGTS-fused* with an APG of 11.08%. In the 14Lap dataset, *Trans-ASTE* achieves an APG value of 17.39% in F1 compared to *BARTABSA-fused*, and 14.61% over *MiniConGTS-fused*. For the 15Res dataset, *Trans-ASTE* maintains a high level of performance, with an F1 score (91.11%) slightly leading both baselines. The overall F1 improvement is 0.34% com-

¹APG = Metric (Our Model) – Metric (Baseline)

Models	14Res			14Lap			15res			16res		
	P	R	F1	P	R	F1	P	R	F1	P	R	F1
CMLA+(Wang et al., 2017) \diamond	-	-	48.95	-	-	44.10	-	-	44.60	-	-	50.00
Peng-two-stage (Peng et al., 2020) \diamond	-	-	56.10	-	-	53.85	-	-	56.23	-	-	60.04
Dual-MRC (Mao et al., 2021) \diamond	-	-	74.93	-	-	63.37	-	-	64.97	-	-	75.71
SpanMlt (Zhao et al., 2020) \bullet	-	-	75.60	-	-	68.66	-	-	64.68	-	-	71.78
BARTABSA (Yan et al., 2021) \diamond	-	-	77.68	-	-	66.11	-	-	67.98	-	-	<u>77.38</u>
MiniConGTS (Sun et al., 2024) \star	-	-	<u>79.60</u>	-	-	<u>73.23</u>	-	-	<u>73.87</u>	-	-	76.29
SOTAs on fused dataset												
BARTABSA-fused	75.40	76.76	76.07	72.36	63.40	67.59	88.85	92.77	90.77	87.06	87.32	87.19
MiniConGTS-fused	81.06	78.82	79.92	75.62	71.61	73.56	93.63	92.72	93.17	78.80	81.82	80.28
Ours on fused dataset												
Trans-AOPE ($w_1:w_2 = 1:1$)	91.88	80.83	86.00	85.87	74.68	79.89	94.88	88.25	91.45	94.63	89.10	91.80
Trans-AOPE ($w_1:w_2 = 1:0$)	93.80	80.39	86.58	88.60	74.26	80.80	95.07	88.95	91.91	93.10	89.01	91.01

Table 3: Comparison of different models on multiple datasets for AOPE task. Recall and precision values are omitted where they are not provided. Former best scores are underlined, and current best scores are bold. \diamond are retrieved from Yan et al., 2021. \bullet is retrieved from Zhao et al., 2020, and \star are retrieved from Sun et al., 2024

Models	14Res			14Lap			15Res			16Res		
	P	R	F1	P	R	F1	P	R	F1	P	R	F1
Peng-Two-stage (Peng et al., 2020) \star	43.24	63.66	51.46	38.87	50.38	42.87	48.07	57.51	52.32	46.96	64.24	54.21
BARTABSA (Yan et al., 2021) \diamond	65.52	64.99	65.25	61.41	56.19	58.69	59.14	59.38	59.26	66.60	68.68	67.62
GTS (Wu et al., 2020) \star	67.76	67.29	67.50	57.82	51.32	54.36	62.59	57.94	60.15	66.08	66.91	67.93
JET-BERT (Xu et al., 2020) \star	70.56	55.94	62.40	55.39	43.57	51.04	64.45	51.96	57.53	70.42	58.37	63.83
COM-MRC (Zhai et al., 2022) \star	75.46	68.91	72.01	58.15	60.17	61.17	68.35	61.24	64.53	71.55	71.59	71.57
EMC-GCN (Chen et al., 2022) \star	71.21	72.39	71.78	61.70	56.26	58.81	61.54	62.47	61.93	65.62	71.30	68.33
BDTF (Chen et al., 2022) \star	75.53	73.24	74.35	68.94	55.97	61.74	68.76	63.71	66.12	71.44	73.13	72.27
DGCNAP (Li et al., 2023) \star	72.90	68.69	70.72	62.02	53.79	57.57	62.23	60.21	61.19	69.75	69.44	69.58
Triple-MRC (Zou et al., 2024) \star	-	-	72.45	-	-	60.72	-	-	62.86	-	-	68.65
STAGE-3D (Liang et al., 2023) \star	<u>78.58</u>	69.58	73.76	71.98	53.86	61.58	<u>73.63</u>	57.90	64.79	<u>76.67</u>	70.12	73.24
MiniConGTS (Sun et al., 2024) \star	76.10	<u>75.08</u>	<u>75.59</u>	66.82	<u>60.68</u>	<u>63.61</u>	66.50	<u>63.86</u>	<u>65.15</u>	75.52	<u>74.14</u>	<u>74.83</u>
SOTAs on fused dataset												
BARTABSA-fused	71.05	72.33	71.68	63.66	56.01	59.59	88.98	92.77	90.77	83.82	84.07	83.95
MiniConGTS-fused	73.89	72.84	73.36	68.26	57.42	62.37	90.64	89.32	89.98	72.73	73.21	72.97
Ours												
Trans-ASTE ($w_1:w_2 = 1:1$)	89.30	77.10	82.76	83.81	69.64	76.07	93.80	86.71	90.11	92.18	86.81	89.42
Trans-ASTE ($w_1:w_2 = 1:0$)	91.70	78.24	84.44	84.63	70.59	76.98	94.31	88.11	91.11	92.78	87.58	90.11

Table 4: Comparison of different models on multiple datasets for ASTE task. Former best scores are underlined, and current best scores are bold. \star are retrieved from Sun et al., 2024, and \diamond is retrieved from Yan et al., 2021.

pared to *BARTABSA-fused* and 1.13% compared to *MiniConGTS-fused*. The 16Res dataset also sees consistently high performance from *Trans-ASTE*), with the highest F1 score (90.11%), representing an APG of 6.16% over *BARTABSA-fused*.

Overall, combining datasets for all-for-one training does not always result in performance improvements across all datasets for SOTA models. However, when data is fused for our model, it consistently achieves performance gains across datasets, with significant improvements observed in 14Res, 14Lap, and 16Res. That said, the slightly lower performance on the 15Res AOPE task highlights potential areas for further optimization in specific scenarios.

5 Conclusion

In this paper, we present an efficient transition pipeline for aspect-opinion pair extraction with linear time complexity $O(n)$, enhanced by a contrastive learning-based optimization method. This approach eliminates the need to directly identify and extract individual tokens, avoiding token-level bias. It can be trained on datasets with the most comprehensive coverage of the designed actions, resulting in significant performance improvements across various datasets. Specifically, training our model on a well-covered fused dataset enables it to learn robust action combination patterns, leading to superior performance on all datasets. Our model surpasses SOTA models on the same fused dataset,

setting new benchmarks for AOPE and ASTE tasks. This approach not only enhances model efficiency but also demonstrates its effectiveness and versatility in improving performance.

Limitation

The primary limitation of the transition-based pipeline lies in its reliance on relatively large and diverse datasets to effectively learn action patterns. As evidenced by the findings in Figure 3, the model achieved better performance on the 15res test set when trained on datasets like 14res and 16res, which appear to provide richer and more diverse action patterns compared to the 15res training set. This observation highlights the inadequacy of relying solely on a single dataset, as it may lack the breadth and complexity needed to capture the full spectrum of action patterns required for robust model generalization. Without access to such diverse training data, the model’s ability to adapt to nuanced patterns or unseen contexts in the test data may be significantly compromised, emphasizing the importance of training on a fused or broader dataset to enhance its overall effectiveness.

References

- Alfred V Aho and Jeffrey D Ullman. 1973. *The theory of parsing, translation, and compiling*, volume 1. Prentice-Hall Englewood Cliffs, NJ.
- Jianzhu Bao, Chuang Fan, Jipeng Wu, Yixue Dang, Jiachen Du, and Ruifeng Xu. 2021. A neural transition-based model for argumentation mining. In *Proceedings of the 59th Annual Meeting of the Association for Computational Linguistics and the 11th International Joint Conference on Natural Language Processing (Volume 1: Long Papers)*, pages 6354–6364.
- Erik Cambria, Soujanya Poria, Alexander Gelbukh, and Mike Thelwall. 2017. Senticnet 5: Discovering conceptual primitives for sentiment analysis by means of context embeddings. In *Proceedings of AAAI*.
- Daniel M Cer, Marie-Catherine De Marneffe, Daniel Jurafsky, and Christopher D Manning. 2010. Parsing to stanford dependencies: Trade-offs between speed and accuracy. In *LREC*. Floriana, Malta.
- Abir Chakraborty. 2024. [Aspect and opinion term extraction using graph attention network](#). *Preprint*, arXiv:2404.19260.
- Hao Chen, Zepeng Zhai, Fangxiang Feng, Ruifan Li, and Xiaojie Wang. 2022. Enhanced multi-channel graph convolutional network for aspect sentiment triplet extraction. In *Proceedings of the 60th Annual Meeting of the Association for Computational Linguistics (Volume 1: Long Papers)*, pages 2974–2985.
- Benjamin Eysenbach, Tianjun Zhang, Ruslan Salakhutdinov, and Sergey Levine. 2023. [Contrastive learning as goal-conditioned reinforcement learning](#). *Preprint*, arXiv:2206.07568.
- Daniel Fernández-González. 2023. [Structured sentiment analysis as transition-based dependency parsing](#). *Preprint*, arXiv:2305.05311.
- Alex Graves and Jürgen Schmidhuber. 2005. Framewise phoneme classification with bidirectional lstm and other neural network architectures. *Neural networks*, 18(5-6):602–610.
- Carlos Gómez-Rodríguez, Michalina Strzyz, and David Vilares. 2020. [A unifying theory of transition-based and sequence labeling parsing](#). *Preprint*, arXiv:2011.00584.
- Sepp Hochreiter and Jürgen Schmidhuber. 1997. [Long short-term memory](#). *Neural Comput.*, 9(8):1735–1780.
- Matthew Honnibal, Ines Montani, Sofie Van Landeghem, and Adriane Boyd. 2020. [spacy: Industrial-strength natural language processing in python](#).
- Yiren Jian, Chongyang Gao, and Soroush Vosoughi. 2022. [Contrastive learning for prompt-based few-shot language learners](#). *Preprint*, arXiv:2205.01308.
- Baoxing Jiang, Shehui Liang, Peiyu Liu, Kaifang Dong, and Hongye Li. 2023. [A semantically enhanced dual encoder for aspect sentiment triplet extraction](#). *Preprint*, arXiv:2306.08373.
- Yanbo Li, Qing He, and Damin Zhang. 2023. Dual graph convolutional networks integrating affective knowledge and position information for aspect sentiment triplet extraction. *Frontiers in Neurobotics*, 17:1193011.
- Shuo Liang, Wei Wei, Xian-Ling Mao, Yuanyuan Fu, Rui Fang, and Danyang Chen. 2023. Stage: span tagging and greedy inference scheme for aspect sentiment triplet extraction. In *Proceedings of the AAAI Conference on Artificial Intelligence*, volume 37, pages 13174–13182.
- Yaxin Liu, Yan Zhou, Ziming Li, Dongjun Wei, Wei Zhou, and Songlin Hu. 2022. Mrce: A multi-representation collaborative enhancement model for aspect-opinion pair extraction. In *International Conference on Neural Information Processing*, pages 260–271. Springer.
- Yinhan Liu, Myle Ott, Naman Goyal, Jingfei Du, Mandar Joshi, Danqi Chen, Omer Levy, Mike Lewis, Luke Zettlemoyer, and Veselin Stoyanov. 2019. [Roberta: A robustly optimized bert pretraining approach](#). *Preprint*, arXiv:1907.11692.
- Yue Mao, Yi Shen, Chao Yu, and Longjun Cai. 2021. A joint training dual-mrc framework for aspect based sentiment analysis. In *Proceedings of the AAAI conference on artificial intelligence*, volume 35, pages 13543–13551.

- Joakim Nivre. 2003. [An efficient algorithm for projective dependency parsing](#). In *Proceedings of the Eighth International Conference on Parsing Technologies*, pages 149–160, Nancy, France.
- Haiyun Peng, Lu Xu, Lidong Bing, Fei Huang, Wei Lu, and Luo Si. 2020. [Knowing what, how and why: A near complete solution for aspect-based sentiment analysis](#). *Proceedings of the AAAI Conference on Artificial Intelligence*, 34(05):8600–8607.
- Maria Pontiki, Dimitris Galanis, Haris Papageorgiou, Ion Androutsopoulos, Suresh Manandhar, Mohammad AL-Smadi, Mahmoud Al-Ayyoub, Yanyan Zhao, Bing Qin, Orphée De Clercq, Véronique Hoste, Marianna Apidianaki, Xavier Tannier, Natalia Loukachevitch, Evgeniy Kotelnikov, Nuria Bel, Salud María Jiménez-Zafra, and Gülşen Eryiğit. 2016. [SemEval-2016 task 5: Aspect based sentiment analysis](#). In *Proceedings of the 10th International Workshop on Semantic Evaluation (SemEval-2016)*, pages 19–30, San Diego, California. Association for Computational Linguistics.
- Maria Pontiki, Dimitris Galanis, Haris Papageorgiou, Suresh Manandhar, and Ion Androutsopoulos. 2015. [SemEval-2015 task 12: Aspect based sentiment analysis](#). In *Proceedings of the 9th International Workshop on Semantic Evaluation (SemEval 2015)*, pages 486–495, Denver, Colorado. Association for Computational Linguistics.
- Maria Pontiki, Dimitris Galanis, John Pavlopoulos, Haris Papageorgiou, Ion Androutsopoulos, and Suresh Manandhar. 2014. [SemEval-2014 task 4: Aspect based sentiment analysis](#). In *Proceedings of the 8th International Workshop on Semantic Evaluation (SemEval 2014)*, pages 27–35, Dublin, Ireland. Association for Computational Linguistics.
- Daniel Rho, TaeSoo Kim, Sooull Park, Jaehyun Park, and JaeHan Park. 2023. [Understanding contrastive learning through the lens of margins](#). *Preprint*, arXiv:2306.11526.
- Qiao Sun, Liujia Yang, Minghao Ma, Nanyang Ye, and Qinying Gu. 2024. [MiniConGTS: A near ultimate minimalist contrastive grid tagging scheme for aspect sentiment triplet extraction](#). In *Proceedings of the 2024 Conference on Empirical Methods in Natural Language Processing*, pages 2817–2834, Miami, Florida, USA. Association for Computational Linguistics.
- Chengwei Wang, Tao Peng, Yue Zhang, Lin Yue, and Lu Liu. 2023. [Aopss: A joint learning framework for aspect-opinion pair extraction as semantic segmentation](#). In *Web and Big Data*, pages 101–113, Cham. Springer Nature Switzerland.
- Wenya Wang, Sinno Jialin Pan, Daniel Dahlmeier, and Xiaokui Xiao. 2017. [Coupled multi-layer attentions for co-extraction of aspect and opinion terms](#). In *Proceedings of the AAAI conference on artificial intelligence*, volume 31.
- Zhen Wu, Chengcan Ying, Fei Zhao, Zhifang Fan, Xinyu Dai, and Rui Xia. 2020. [Grid tagging scheme for aspect-oriented fine-grained opinion extraction](#). *arXiv preprint arXiv:2010.04640*.
- Lu Xu, Hao Li, Wei Lu, and Lidong Bing. 2020. [Position-aware tagging for aspect sentiment triplet extraction](#). *arXiv preprint arXiv:2010.02609*.
- Lu Xu, Hao Li, Wei Lu, and Lidong Bing. 2021. [Position-aware tagging for aspect sentiment triplet extraction](#). *Preprint*, arXiv:2010.02609.
- Hang Yan, Junqi Dai, Tuo Ji, Xipeng Qiu, and Zheng Zhang. 2021. [A unified generative framework for aspect-based sentiment analysis](#). In *Proceedings of the 59th Annual Meeting of the Association for Computational Linguistics and the 11th International Joint Conference on Natural Language Processing (Volume 1: Long Papers)*, pages 2416–2429, Online. Association for Computational Linguistics.
- Kaiyu Yang and Jia Deng. 2020. [Strongly incremental constituency parsing with graph neural networks](#). *Preprint*, arXiv:2010.14568.
- Zepeng Zhai, Hao Chen, Fangxiang Feng, Ruifan Li, and Xiaojie Wang. 2022. [Com-mrc: A context-masked machine reading comprehension framework for aspect sentiment triplet extraction](#). In *Proceedings of the 2022 Conference on Empirical Methods in Natural Language Processing*, pages 3230–3241.
- Meishan Zhang, Yue Zhang, and Guohong Fu. 2016. [Transition-based neural word segmentation](#). In *Proceedings of the 54th Annual Meeting of the Association for Computational Linguistics (Volume 1: Long Papers)*, pages 421–431.
- He Zhao, Longtao Huang, Rong Zhang, Quan Lu, and Hui Xue. 2020. [SpanMlt: A span-based multi-task learning framework for pair-wise aspect and opinion terms extraction](#). In *Proceedings of the 58th Annual Meeting of the Association for Computational Linguistics*, pages 3239–3248, Online. Association for Computational Linguistics.
- Jiawei Zhou, Tahira Naseem, Ramón Fernandez Astudillo, Young-Suk Lee, Radu Florian, and Salim Roukos. 2021. [Structure-aware fine-tuning of sequence-to-sequence transformers for transition-based amr parsing](#). *Preprint*, arXiv:2110.15534.
- Wang Zou, Wubo Zhang, Wenhuan Wu, and Zhuoyan Tian. 2024. [A multi-task shared cascade learning for aspect sentiment triplet extraction using bert-mrc](#). *Cognitive Computation*, pages 1–18.

A Appendix

A.1 Alternative Solution with State Changes

Since stack can hold more than two tokens, "is" can be moved to stack ($\beta_3 \rightarrow \sigma_3$) before "Gourmet" and "food" merge ($[\sigma_1, \sigma_2, \sigma_3] \rightarrow [\sigma_{1\&2}, \sigma_3]$). The detailed process is present in Table 5.

Phrase	Action	Stack (σ)	Buffer (β)	Aspect	Opinion	Pair
–	–	[]	$[\beta_1, \beta_2, \beta_3, \beta_4]$	–	–	–
1	<i>SF</i>	$[\sigma_1]$	$[\beta_2, \beta_3, \beta_4]$	–	–	–
2	<i>SF</i>	$[\sigma_1, \sigma_2]$	$[\beta_3, \beta_4]$	–	–	–
3	<i>SF</i>	$[\sigma_1, \sigma_2, \beta_3]$	$[\beta_4]$	–	–	–
4	<i>M</i>	$[\sigma_{1\&2}, \beta_3]$	$[\beta_4]$	–	–	–
5	<i>R_n</i>	$[\sigma_{1\&2}]$	$[\beta_4]$	–	–	–
6	<i>SF</i>	$[\sigma_{1\&2}, \sigma_4]$	[]	–	–	–
7	<i>RR</i>	$[\sigma_{1\&2}, \sigma_4]$	[]	$[\sigma_{1\&2}]$	$[\sigma_4]$	$(\sigma_{1\&2} \rightarrow \sigma_4)$
9	<i>ST</i>	[]	[]	$[\sigma_{1\&2}]$	$[\sigma_4]$	$(\sigma_{1\&2} \rightarrow \sigma_4)$

Table 5: State changes for "Gourmet food is delicious" using symbolic representation. Here, σ_1 corresponds to "Gourmet", σ_2 to "food", σ_3 to "is", and σ_4 to "delicious". Similarly, $\beta_1, \beta_2, \beta_3,$ and β_4 correspond to tokens in the buffer in sequence.

A.2 Algorithm for Transition Actions

In Algorithm 1, while the core of the algorithm focuses on the action operations, the configuration also plays a vital role in its functionality.

The algorithm begins with a buffer, a list of input tokens representing the text to be parsed. These tokens are consumed during the parsing process and form the basis for token pair relationships. A critical component of the algorithm is the pair2sent mapping, which associates token pairs with their corresponding sentiment labels, allowing the algorithm to enrich the output with sentiment information, even for token pairs not explicitly provided in the target data (defaulting to a neutral label). Then, each parsing action (e.g., Shift, Left Relation, Right Relation) is mapped to a unique numeric ID. This mapping enables a compact representation of the sequence of parsing actions, which is useful for downstream tasks like training or evaluation. Throughout the parsing process, the algorithm records intermediate states (stack, buffer, actions, and sentiment labels) to maintain a complete history of its operations. Simultaneously, valid token pairs are stored in pairs, capturing the structured relationships in the text.

A.3 Action Coverage on Different Datasets

The coverage of actions, as shown in Table 6, reveals some differences in the recall values across data sets. The 14Lap and 14Res datasets exhibit lower recall compared to the 15Res and 16Res datasets. This trend is observed across training, development, and testing phases, with recall values for 14 datasets remaining around 85-87%, while 15Res and 16Res achieve significantly higher recalls, exceeding 91% in most cases. The fused

	14lap	14res	15res	16res	fused
train (Precision)	99.99	99.99	99.99	99.99	99.99
train (Recall)	85.51	86.63	92.98	93.04	88.73
train (F1)	92.19	92.84	96.36	96.40	94.03
dev (Precision)	99.99	99.99	99.99	99.99	99.99
dev (Recall)	85.97	86.89	94.92	93.04	89.88
dev (F1)	92.46	92.99	97.39	96.40	94.67
test (Precision)	99.99	99.99	99.99	99.99	99.99
test (Recall)	86.66	87.54	91.47	92.42	89.41
test (F1)	92.85	93.36	95.54	96.06	94.41
total (Precision)	99.99	99.99	99.99	99.99	99.99
total (Recall)	86.02	87.03	92.56	92.79	89.00
total (F1)	92.48	93.06	96.14	96.26	94.18

Table 6: Transposed Transitional Action Coverage for 14Lap, 14Res, 15Res, 16Res, and fused Datasets.

dataset strikes a balance with intermediate recall values, reflecting the integration of characteristics from all datasets. This highlights a relative weakness in capturing relevant actions in 14 datasets compared to 15 and 16 datasets.

A.4 Growth with Different Optimization Weight

Figures 6 and 7, 8 and 9, and 10 and 11 depict the performance growth with varying weights applied to the 14res, 15res, and 16res datasets, respectively. These figures highlight the influence of weight adjustments on model accuracy and efficiency in ASTE tasks. By examining the trends across these datasets, we demonstrate the early benefits of augmented optimization in enhancing performance.

Algorithm 1 Argument-Opinion Pair Parsing Algorithm

Require: buffer (list of input tokens), pair2sent (mapping of token pairs to sentiment labels), action2id (mapping of parsing actions to numeric IDs)

Ensure: states (list of recorded parsing states), pairs (list of valid token pairs)

```
1: Initialize empty stack, actions, states, and pairs.
                                     ▷ Main processing loop: parse tokens from the buffer
2: while buffer is not empty do
3:   if len(stack) < 2 then
4:     stack.append(buffer.pop(0))                                     ▷ Apply SH: Shift
5:     Append SF to actions.
6:     continue
7:   end if
                                     ▷ Form a pair from the top two elements in stack
8:   stackPair ← (stack[-2], stack[-1])
9:   currentAction ← getAction(stackPair, targetPairs)
10:  Append currentAction to actions.
                                     ▷ Handle relation formation actions (LR and RR)
11:  if currentAction == LR then
12:    Add stackPair to pairs.
13:    sentimentLabel ← pair2sent.get(stackPair, 3)
14:    Apply stack[-2] and stack[-1] form a left-relation pair.
15:  else if currentAction == RR then
16:    Add stackPair to pairs.
17:    sentimentLabel ← pair2sent.get(stackPair, 3)
18:    Apply stack[-1] and stack[-2] form a right-relation pair.
19:  else
20:    sentimentLabel ← 3                                             ▷ Default sentiment label.
21:  end if
                                     ▷ Record the current parsing state
22:  Record (stack, buffer, actions, sentimentLabel) in states.
                                     ▷ Modify the stack based on currentAction
23:  if currentAction ==  $L_n$  then
24:    Remove stack[-2]                                             ▷ Apply  $L_n$ : Left Constituent Removal
25:  else if currentAction ==  $R_n$  then
26:    Remove stack[-1]                                             ▷ Apply  $R_n$ : Right Constituent Removal
27:  else if currentAction == M then
28:    Merge stack[-2] and stack[-1]                                 ▷ Apply M: Merge
29:  end if
30: end while
                                     ▷ Finalize by reducing the remaining elements in the stack
31: while len(stack) > 1 do
32:   Remove the top element from stack                               ▷ Apply ST: Stop
33: end while
                                     ▷ Convert actions to numeric IDs for output
34: Map each action in states to its ID using action2id.
    return states, pairs.
```

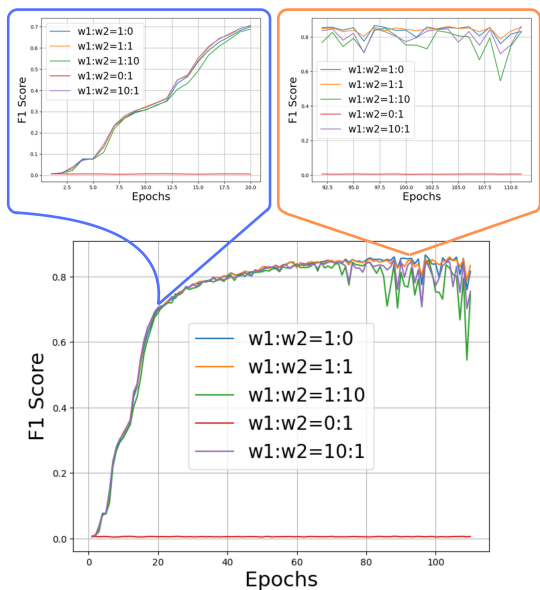


Figure 6: Growth on different weights for AOPE task on 14res testing set.

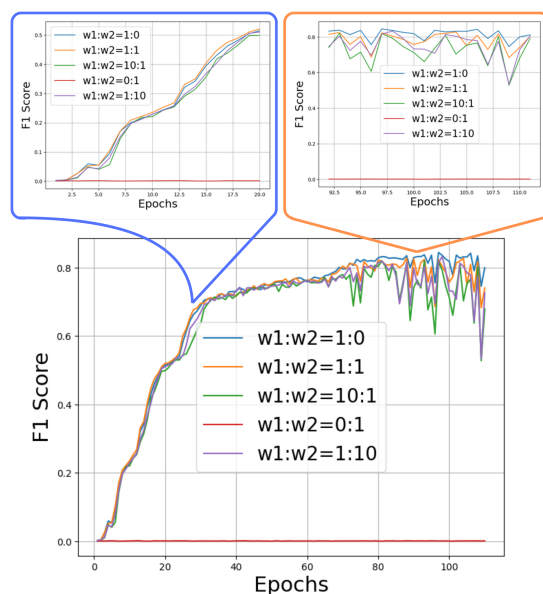


Figure 7: Growth on different weights for ASTE task on 14res testing set.

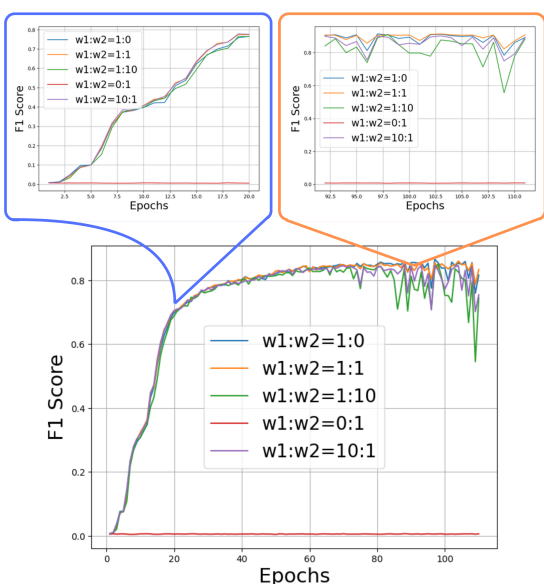


Figure 8: Growth on different weights for AOPE task on 15res testing set.

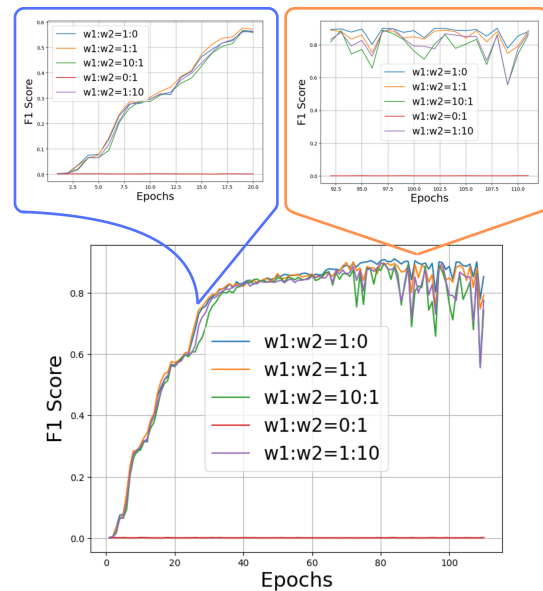


Figure 9: Growth on different weights for ASTE task on 15res testing set.

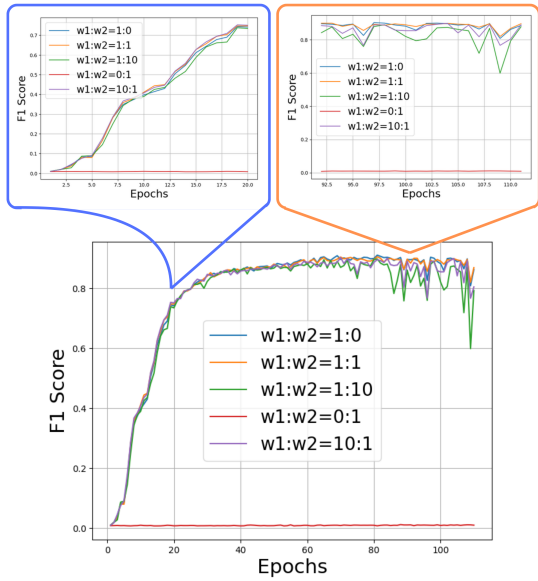


Figure 10: Growth on different weights for AOPe task on 16res testing set.

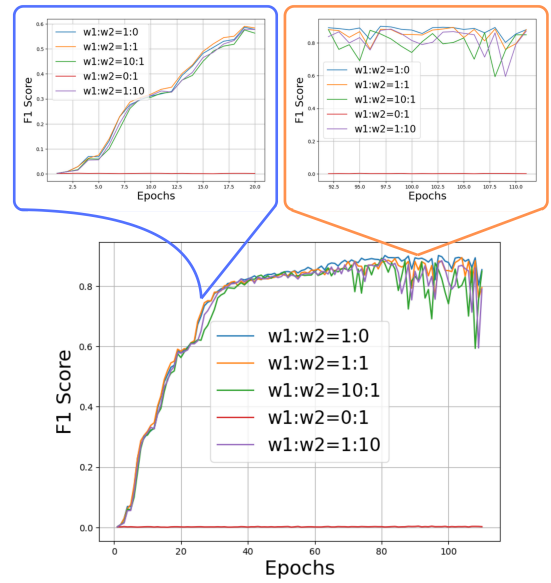


Figure 11: Growth on different weights for ASTE task on 16res testing set.

A.5 Growth Comparison for AOPe and ASTE

The growth comparison for AOPe and ASTE is illustrated in Figures 12, 13, 14, and 15, corresponding to the 14res, 14lap, 15res, and 16res datasets, respectively. While ASTE generally follows the trends observed in AOPe, the fluctuations in ASTE are more extreme. These figures emphasize the sensitivity of ASTE to variations in model weights or dataset conditions, which results in sharper peaks and deeper troughs compared to the relatively smoother patterns seen in AOPe. This highlights the unique challenges posed by the ASTE task across different datasets.

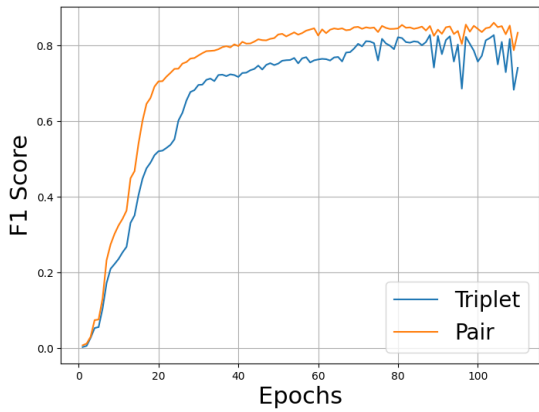


Figure 12: Growth Comparison for AOPE and ASTE on 14res Testing set.

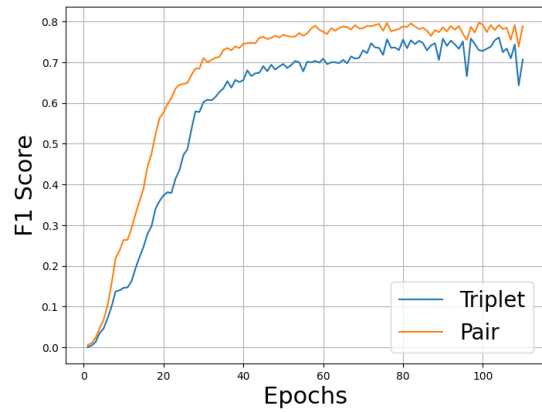


Figure 13: Growth Comparison for AOPE and ASTE on 14lap Testing set.

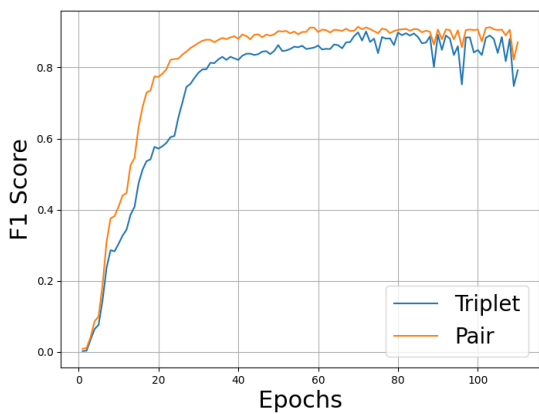


Figure 14: Growth Comparison for AOPE and ASTE on 15res Testing set.

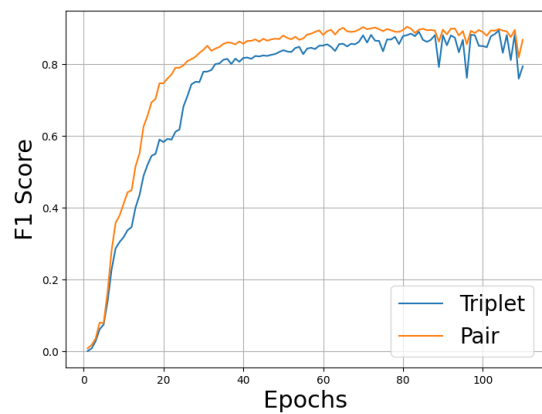


Figure 15: Growth Comparison for AOPE and ASTE on 16res Testing set.